

Large Deviation Analysis of Score-based Hypothesis Testing

Enmao Diao, Taposh Banerjee, *Member, IEEE*, and Vahid Tarokh, *Fellow, IEEE*

Abstract—Score-based statistical models play an important role in modern machine learning, statistics, and signal processing. For hypothesis testing, a score-based hypothesis test is proposed in [1]. We analyze the performance of this score-based hypothesis testing procedure and derive upper bounds on the probabilities of its Type I and II errors. We prove that the exponents of our error bounds are asymptotically (in the number of samples) tight for the case of simple null and alternative hypotheses. We calculate these error exponents explicitly in specific cases and provide numerical studies for various other scenarios of interest.

I. INTRODUCTION

Score matching [2, 3] is a procedure that has emerged due to its ability to outperform likelihood-based benchmarks in image generations [4, 5]. It has been shown that it is possible to efficiently model $\nabla \log p(x)$ using deep neural networks (DNNs), where $p(x)$ denotes the data generating density. However, it is computationally non-trivial to calculate even un-normalized versions of $p(x)$ from these trained DNNs. For log-likelihood-based hypothesis testing and change detection, there exists a well-established literature. Recently change detection and hypothesis testing for score-based systems have been studied. In particular, score-based hypothesis testing [1] was proposed as a procedure to decide whether or not to reject a hypothesis. We note that the likelihood ratio test (LRT) is a standard method commonly used for hypothesis testing, and the celebrated Neyman-Pearson lemma gives the uniformly most powerful optimality property of LRT for simple hypotheses testing. This implies that score-based hypothesis testing cannot outperform the LRT test for simple hypotheses testing when the densities of data under the null and alternative hypotheses are exactly known. However, the evaluation of exact likelihoods may be computationally cumbersome (or even intractable) for various modern statistical models including graphical models [6], energy-based models [7] and deep generative models [8]. This gives some importance to score-based hypothesis testing [1] and the analysis of its performance. This motivates our work in this paper, where we derive upper bounds on the probabilities of its Type I and II errors for score-based hypothesis testing, and establish that the exponents of our error bounds are asymptotically (in the number of samples) tight for the case of simple null and alternative hypotheses.

Enmao Diao and Vahid Tarokh are with the Department of Electrical and Computer Engineering, Duke University, Durham, NC 27708, USA. Taposh Banerjee is with the Department of Industrial Engineering, University of Pittsburgh, PA 15213, USA. Vahid Tarokh was supported in part by Air Force Research Lab grant number FA-8750-20-2-0504. Taposh Banerjee was supported in part by the U.S. Army Research Lab under grant W911NF2120295.

The outline of our paper is given next. In Section II, we will motivate the problem to be considered in this paper, review the related work, and present the score-based test for binary hypothesis testing [1]. We then derive upper bounds on the probabilities of its Type I and II errors for finite sample size in Section III. In Section IV, we show that these bounds are asymptotically tight using large deviation theory [9, 10]. In Section V, we discuss simulation methods for estimating these error exponents. In Section VI, we provide explicit calculation for the error exponent in the multivariate Gaussian case. In Section VII, we show the accuracy of these error bounds for experiments performed on real and simulated data. We will make our concluding remarks in Section VIII.

II. SCORE-BASED HYPOTHESIS TESTING FOR UNNORMALIZED STATISTICAL MODELS

A. Binary Hypothesis Testing

Let $x \in \mathcal{X} \subseteq \mathbb{R}^d$ be the realization of a random vector X . We denote $\mathbf{X}_n \triangleq \{X_1, \dots, X_n\}$ as independent and identically distributed (i.i.d.) observations from an unknown distribution P with probability density p . For two probability measures P_∞ and P_1 with respective densities p_∞ and p_1 , we investigate the simple binary hypotheses testing problem:

$$\mathcal{H}_0 : p = p_\infty \quad \text{against} \quad \mathcal{H}_1 : p = p_1. \quad (1)$$

It is well-known that the optimal test in Bayesian, minimax, and variational settings is the likelihood ratio test (LRT):

$$\delta_L(X) = \begin{cases} 1, & \text{if } S_L(\mathbf{X}_n, p_\infty) - S_L(\mathbf{X}_n, p_1) > T \\ 0 & \text{otherwise.} \end{cases} \quad (2)$$

Here,

$$S_L(\mathbf{X}_n, p) = -\log \prod_{i=1}^n p(X_i).$$

is the log score of the sample (X_1, \dots, X_n) . The choice of the threshold T depends on the problem formulation. In the variational setting of Neymann and Pearson, the threshold is chosen to set the type-I error. The performance and optimality properties of this test can be found in most standard texts; see, for example, [11, 12]. When the densities p_∞ and p_1 are not known, the LRT statistic is replaced by a suitable statistic depending on the assumptions on the data. Such families of tests include the generalized likelihood ratio (GLR) test, mixture tests, and nonparametric tests [12, 13].

B. Limitations of the LRT for Score-Based Models

In modern machine learning applications, two new classes of models have emerged:

- 1) *Unnormalized statistical models*: In these models, we know the densities p_∞ and p_1 within normalizing constants. Specifically, we have

$$p_\infty(x) = \frac{\tilde{p}_\infty(x)}{Z_\infty}, \quad \text{and} \quad p_1(x) = \frac{\tilde{p}_1(x)}{Z_1}. \quad (3)$$

Here

$$Z_\infty = \int_x \tilde{p}_\infty(x) dx, \quad \text{and} \quad Z_1 = \int_x \tilde{p}_1(x) dx. \quad (4)$$

are normalizing constants that are hard (or even impossible) to calculate by numerical integration. The unnormalized models $\tilde{p}_\infty(x)$ and $\tilde{p}_1(x)$ are known in precise functional forms. Examples include continuous-valued Markov random fields or undirected graphical models which are used for image modeling [2, 14]. In this case, the LRT can still be implemented. This is because the LRT can be written as

$$\begin{aligned} \delta_L(X) &= \begin{cases} 1, & \text{if } \prod_{i=1}^n \frac{p_1(X_i)}{p_\infty(X_i)} > T \\ 0 & \text{otherwise,} \end{cases} \\ &= \begin{cases} 1, & \text{if } \prod_{i=1}^n \frac{\tilde{p}_1(X_i)}{\tilde{p}_\infty(X_i)} > T_1 \\ 0 & \text{otherwise.} \end{cases} \end{aligned} \quad (5)$$

Here $T_1 = \left(\frac{Z_1}{Z_\infty}\right)^n T$. If T_1 is chosen to satisfy a constraint on the type-I error (which can be done by sampling from p_∞ using its unnormalized version \tilde{p}_∞), then the LRT test can still be implemented.

- 2) *Score-based models*: In many modern machine learning applications, even $\tilde{p}_\infty(x)$ and $\tilde{p}_1(x)$ are unknown. But, we may learn the scores,

$$\nabla_x \log p_\infty(x) \quad \text{and} \quad \nabla_x \log p_1(x),$$

from data. This is possible using the idea of *score-matching*. Specifically, these scores can be learned using a deep neural network [2, 4, 14, 15, 16, 17]. We note that a score-based model is also unnormalized where the exact form of the unnormalized function is hard to estimate. In this case, the LRT cannot be implemented and a fresh approach is needed.

C. Score-Based Hypothesis Testing

A score-based approach to hypothesis testing was taken in [1]. This test was based on the concept of Hyvärinen Score [2]. To define this score and the corresponding test, let p and q be two probability densities defined on \mathcal{X} . The Fisher divergence between p and q is defined as

$$\mathbb{D}_F(p \parallel q) \triangleq \mathbb{E}_{X \sim p} \left[\frac{1}{2} \|\nabla_x \log p(X) - \nabla_x \log q(X)\|_2^2 \right], \quad (6)$$

whenever the integral is well defined. Under some mild regularity conditions on p and q [2], the Fisher divergence can be rewritten as

$$\mathbb{D}_F(p \parallel q) = \mathbb{E}_{X \sim p} \left[\frac{1}{2} \|\nabla_x \log p(X)\|_2^2 + S_H(X, q) \right], \quad (7)$$

with

$$S_H(X, q) \triangleq \frac{1}{2} \|\nabla_x \log q(X)\|_2^2 + \Delta_x \log q(X), \quad (8)$$

where $\Delta_x = \sum_{i=1}^d \frac{\partial^2}{\partial x_i^2}$ denotes the Laplacian operator with respect to $x = (x_1, \dots, x_d)^\top$. The score $S_H(X, q)$ is the Hyvärinen score [2] and is a counterpart of the logarithmic score function $S_L(X, p) = -\log q(X)$ that corresponds to the widely used negative log-likelihood. We further use the notation $S_H(\mathbf{X}_n, p)$ to denote

$$S_H(\mathbf{X}_n, p) \triangleq \frac{1}{n} \sum_{i=1}^n S_H(X_i, p). \quad (9)$$

The score-based test for binary hypothesis testing proposed in [1] is given by

$$\delta(\mathbf{X}_n) = \begin{cases} 1, & \text{if } S_H(\mathbf{X}_n, p_\infty) - S_H(\mathbf{X}_n, p_1) > T \\ 0 & \text{otherwise.} \end{cases} \quad (10)$$

In this paper, we analyze the type-I and type-II error probabilities of this test as $n \rightarrow \infty$ using large deviation theory [9, 10]. In the test of the paper, we drop the subscript H from the $S_H(\mathbf{X}_n, p)$ and simply refer to the Hyvärinen score by $S(\mathbf{X}, p)$ for a collection of n data points and by $S(X, p)$ for a single data point.

Recently, there have been some attempts to perform out-of-distribution (OOD) detection based on score-matching estimates [18, 19]. Note that in OOD detection, the in-distribution samples are assumed to follow a distribution $p(\cdot)$, while the OOD samples are distributed according to another distribution $q(\cdot)$. For an observation x , hypothesis $\mathcal{H}_0 : x \sim p$ is then tested against $\mathcal{H}_1 : x \not\sim p$. In [18], the authors utilized the norm of the gradient of logarithmic likelihood at multiple noise scales for anomaly detection. The authors of [19] estimated the Fisher divergence between the null and alternative distributions for feature shift detection assuming that the data is generated according to the null distribution. In [1], the scores of null distribution and alternative distributions were used to propose a score-based hypothesis test. As we will be analyzing the performance of this method, we will review its required background and subsequently discuss it below.

III. FIXED-SAMPLE ERROR ANALYSIS OF SCORE-BASED TEST FOR BINARY HYPOTHESIS TESTING

Consider the single-sample score-based simple hypotheses test between densities p_∞ and p_1 using n data points $\mathbf{X}_n = (X_1, \dots, X_n)$ (after suppressing the subscript H in (10)):

$$\delta_n \triangleq \delta(\mathbf{X}_n) = \begin{cases} 1, & \text{if } S(\mathbf{X}_n, p_\infty) - S(\mathbf{X}_n, p_1) > T \\ 0 & \text{otherwise,} \end{cases} \quad (11)$$

where recall that $S(\mathbf{X}_n, p) = \frac{1}{n} \sum_{i=1}^n S(X_i, p)$. Thus, choosing $\delta_n = 1$ is interpreted as the selection of the alternative

hypothesis $\mathcal{H}_1 : p = p_1$. The type I error (probability of false alarm) is then given by

$$\alpha_n(\delta_n) \triangleq \mathbb{P}_\infty(\delta_n = 1) = \mathbb{P}_\infty(S(\mathbf{X}_n, p_\infty) - S(\mathbf{X}_n, p_1) > T). \quad (12)$$

This probability can be estimated using Chernoff's bound: for $\theta > 0$

$$\begin{aligned} \alpha_n(\delta_n) &= \mathbb{P}_\infty(S(\mathbf{X}_n, p_\infty) - S(\mathbf{X}_n, p_1) > T) \\ &= \mathbb{P}_\infty\left(\frac{1}{n} \sum_{i=1}^n (S(X_i, p_\infty) - S(X_i, p_1)) > T\right) \\ &= \mathbb{P}_\infty\left(\sum_{i=1}^n (S(X_i, p_\infty) - S(X_i, p_1)) > nT\right) \\ &= \mathbb{P}_\infty\left(e^{\theta(\sum_{i=1}^n (S(X_i, p_\infty) - S(X_i, p_1)))} > e^{n\theta T}\right) \\ &\leq e^{-n\theta T} \mathbb{E}_\infty\left[e^{\theta(\sum_{i=1}^n (S(X_i, p_\infty) - S(X_i, p_1)))}\right] \\ &= \left[e^{-\theta T} e^{\log \mathbb{E}_\infty[e^{\theta(S(X, p_\infty) - S(X, p_1))}]} \right]^n \\ &= \exp\left[n\left(\log \mathbb{E}_\infty\left[e^{\theta(S(X, p_\infty) - S(X, p_1))}\right] - \theta T\right)\right], \end{aligned} \quad (13)$$

where $\mathbb{E}_\infty(\cdot)$ denotes expectation with respect to \mathbb{P}_∞ .

Since this inequality is true for every $\theta > 0$, we can take an infimum over θ on the right-hand side.

$$\begin{aligned} \alpha_n(\delta_n) &\leq \inf_{\theta \geq 0} \exp\left(n \log \mathbb{E}_\infty\left[e^{\theta(S(X, p_\infty) - S(X, p_1))}\right] - \theta T\right) \\ &= \exp\left(n \inf_{\theta \geq 0} \left(\log \mathbb{E}_\infty\left[e^{\theta(S(X, p_\infty) - S(X, p_1))}\right] - \theta T\right)\right) \\ &= \exp\left(-n \sup_{\theta \geq 0} \left(\theta T - \log \mathbb{E}_\infty\left[e^{\theta(S(X, p_\infty) - S(X, p_1))}\right]\right)\right). \end{aligned} \quad (14)$$

Define

$$\phi(\theta) = \log \mathbb{E}_\infty\left[e^{\theta(S(X, p_\infty) - S(X, p_1))}\right].$$

It is well-known that $\phi(\theta)$ is a convex function. Define the Legendre transformation of the convex function $\phi(\theta)$ as

$$\phi^*(T) = \sup_{\theta \geq 0} [\theta T - \phi(\theta)].$$

Thus,

$$\alpha_n(\delta_n) \leq e^{-n\phi^*(T)}, \quad (15)$$

for all $n \geq 1$. Note that $\phi^*(T)$ is strictly positive if T is larger than the slope of $\phi(\theta)$ at $\theta = 0$, which is

$$\begin{aligned} \left.\frac{d}{d\theta} \phi(\theta)\right|_{\theta=0} &= \left.\frac{d}{d\theta} \log \mathbb{E}_\infty\left[e^{\theta(S(X, p_\infty) - S(X, p_1))}\right]\right|_{\theta=0} \\ &= -\mathbb{D}_F(p_\infty \| p_1) < 0. \end{aligned}$$

Thus, for $T > -\mathbb{D}_F(p_\infty \| p_1)$,

$$\alpha_n(\delta_n) \leq e^{-n\phi^*(T)} < 1 \quad (16)$$

for all $n \geq 1$. Thus,

$$\frac{\log \alpha_n(\delta_n)}{n} \leq -\phi^*(T). \quad (17)$$

In the next section, we show that this bound $-\phi^*(T)$ is asymptotically tight using large deviation theory.

We note that a similar argument can be made for the type II error by changing the roles of P_1 and P_∞ . Specifically, we have

$$\begin{aligned} \beta_n(\delta_n) &= \mathbb{P}_1(S(\mathbf{X}_n, p_1) - S(\mathbf{X}_n, p_\infty) > -T) \\ &\leq \exp\left(-n \sup_{\theta \geq 0} \left(-\theta T - \log \mathbb{E}_1\left[e^{\theta(S(X, p_1) - S(X, p_\infty))}\right]\right)\right), \end{aligned} \quad (18)$$

for all $n \geq 1$, where $\mathbb{E}_1(\cdot)$ denotes expectation with respect to \mathbb{P}_1 . We conclude that

$$\frac{\log \beta_n(\delta_n)}{n} \leq -\sup_{\theta \geq 0} \left(-\theta T - \log \mathbb{E}_1\left[e^{\theta(S(X, p_1) - S(X, p_\infty))}\right]\right).$$

IV. LARGE DEVIATION ANALYSIS OF THE SCORE-BASED TEST

By Cramer's theorem [9], the type-I error has a positive error exponent given by

$$\begin{aligned} &\frac{1}{n} \log \mathbb{P}_\infty(\delta_n = 1) \\ &= \frac{1}{n} \log \mathbb{P}_\infty\left(\frac{1}{n} \sum_{i=1}^n (S(X_i, p_\infty) - S(X_i, p_1)) > T\right) \\ &\rightarrow \inf_{\theta \geq 0} \left(\log \mathbb{E}_\infty\left[e^{\theta(S(X_1, p_\infty) - S(X_1, p_1))}\right] - \theta T\right) \\ &= -\sup_{\theta \geq 0} \left(\theta T - \log \mathbb{E}_\infty\left[e^{\theta(S(X_1, p_\infty) - S(X_1, p_1))}\right]\right) \\ &= -\phi^*(T). \end{aligned}$$

Thus, the exponent we calculated in (17) for a sample of size n (using the Chernoff bound) turns out to be tight in the asymptotic regime as $n \rightarrow \infty$.

Similarly, by Cramer's theorem again, the type-II error has a positive error exponent given by

$$\begin{aligned} &\frac{1}{n} \log \mathbb{P}_1(\delta_n = 0) \\ &= \frac{1}{n} \log \mathbb{P}_1\left(\frac{1}{n} \sum_{i=1}^n (S(X_i, p_\infty) - S(X_i, p_1)) < T\right) \\ &= \frac{1}{n} \log \mathbb{P}_1\left(\frac{1}{n} \sum_{i=1}^n (S(X_i, p_1) - S(X_i, p_\infty)) > -T\right) \\ &\rightarrow \inf_{\theta \geq 0} \left(\log \mathbb{E}_1\left[e^{\theta(S(X_1, p_1) - S(X_1, p_\infty))}\right] + \theta T\right) \\ &= -\sup_{\theta \geq 0} \left(-\theta T - \log \mathbb{E}_1\left[e^{\theta(S(X_1, p_1) - S(X_1, p_\infty))}\right]\right). \end{aligned}$$

Let

$$-\mathbb{D}_F(p_\infty \| p_1) < T < \mathbb{D}_F(p_1 \| p_\infty).$$

Then,

$$-T > -\mathbb{D}_F(p_1 \| p_\infty),$$

and this error exponent is also positive.

V. ESTIMATING THE ERROR EXPONENT

The error exponent $\phi^*(T)$ can be estimated empirically by using numerical simulation to design the hypothesis test. Since we have access to the score $\nabla \log p_\infty(x)$, we can sample from it using Markov Chain Monte Carlo (MCMC) techniques such as Metropolis Adjusted Langevin Algorithm (MALA), Hamiltonian Monte Carlo (HMC), etc. Let X_1, X_2, \dots, X_m be m samples generated using such an MCMC Algorithm. Then the function of θ given by

$$\theta T - \log \mathbb{E}_\infty \left[e^{\theta(S(X_1, p_\infty) - S(X_1, p_1))} \right]$$

can be empirically estimated by

$$\theta T - \log \frac{1}{m} \sum_{k=1}^m \left[e^{\theta(S(X_k, p_\infty) - S(X_k, p_1))} \right].$$

The above expression can be optimized over θ using standard gradient descent algorithms in order to estimate $\phi^*(T)$. The error exponent for type II error can be numerically calculated in an analogous manner.

VI. EXPLICIT CALCULATION FOR SPECIFIC CASES

We note that for some specific distributions, the above error exponents can be calculated in closed form. As an example, we consider the standard simple Gaussian hypothesis testing with where the null and alternative hypothesis have the same co-variance matrices. Without loss of generality, we can assume that P_∞ is multidimensional Gaussian $N(0, \Sigma)$ with mean zero and co-variance matrix Σ and P_1 is $N(\mu, \Sigma)$. Then by direct calculation:

$$S(X, p_\infty) - S(X, p_1) = -\frac{\mu^T}{2} \Sigma^{-2} (X - \frac{\mu}{2}).$$

Another straightforward calculation gives

$$\begin{aligned} \mathbb{E}_\infty \left[e^{\theta(S(X, p_\infty) - S(X, p_1))} \right] &= \mathbb{E}_\infty \left[e^{-\theta \frac{\mu^T}{2} \Sigma^{-2} (X - \frac{\mu}{2})} \right] \\ &= e^{\theta \frac{\mu^T \Sigma^{-2} \mu}{4}} e^{\theta^2 \frac{\mu^T \Sigma^{-3} \mu}{8}}. \end{aligned} \quad (19)$$

We thus have

$$\begin{aligned} \theta T - \log \mathbb{E}_\infty \left[e^{\theta(S(X, p_\infty) - S(X, p_1))} \right] \\ = \theta T - \theta \frac{\mu^T \Sigma^{-2} \mu}{4} - \theta^2 \frac{\mu^T \Sigma^{-3} \mu}{8}. \end{aligned} \quad (20)$$

If $T < \frac{\mu^T \Sigma^{-2} \mu}{4}$ then the maxima is achieved at $\theta = 0$ and the type I error exponent is given by $\phi^*(T) = 0$. Otherwise, the maxima is achieved at $\theta = \frac{4T - \mu^T \Sigma^{-2} \mu}{\mu^T \Sigma^{-3} \mu}$ and the type I error exponent is given by

$$\phi^*(T) = \frac{(4T - \mu^T \Sigma^{-2} \mu)^2}{8\mu^T \Sigma^{-3} \mu},$$

which is quadratic in T , which is the same behavior as the log-likelihood ratio test.

VII. NUMERICAL EXPERIMENTS

In this section, numerical experiments are conducted using various datasets in order to numerically demonstrate the effectiveness of our large deviation analysis of score-based hypothesis testing. Our experiments utilize both synthetic and real-world data.

- 1) *Synthetic datasets*: For synthetic datasets, we consider samples generated from multivariate normal distributions, exponential family, and Gauss-Bernoulli Restricted Boltzmann Machines (RBMs) [1]. When the exact likelihood is available, as in the case of multivariate normal distributions and the exponential family, we compare the performance of the Hyvarinen Score Test (HST) with that of the Likelihood Ratio Test (LRT). For each distribution type, we perform 10 runs, with each run producing a datasets of size 10,000 created by sampling from both the null and alternative distributions.
- 2) *Real datasets*: For real-world datasets, we utilize the KDD Cup'99 dataset [20]. This dataset contains various types of simulated adversarial network attacks and is typically used for bench-marking network intrusion detection algorithms.

For all experiments, we evaluate the *Positive Error Exponent* (for Type I error) and *Negative Error Exponent* (for Type II error) for various thresholds. Using numerical calculations, we compare the estimates of the theoretical results obtained from the large deviation analysis given above, with the empirical error exponent obtained from hypothesis tests of size n by sampling with replacement (ranging from $n = 1$ to $n = 128$). The threshold for calculating the theoretical limit is obtained empirically with $n = 1$.

A. Details of Experimental Setup

We now discuss the experiments in detail.

a) *Multivariate normal distribution*: For the multivariate normal distribution data, we consider the bivariate normal distribution $\mathcal{N}(\mu, \Sigma)$, performing tests on μ with known Σ , and vice versa. The null hypothesis P_∞ is: The mean μ_0 (respectively the covariance Σ_0) is equal to its true value μ^* (or Σ^*). The corresponding values of the alternative hypothesis P_1 are assigned by adding i.i.d. samples of a noise term $\mathcal{N}(0, \sigma_{ptb}^2)$ to coordinates of μ_∞ (or by adding a i.i.d. samples of a log-Normal noise to diagonal elements of Σ_∞ , where the logarithm of each noise term is distributed according to a Normal distribution $\mathcal{N}(0, \sigma_{ptb}^2)$). In our simulations, we let $\mu_\infty = (0, 0)^T$ (respectively $\Sigma_\infty = \begin{bmatrix} 1 & 0.7 \\ 0.7 & 1 \end{bmatrix}$) for the null hypotheses in each trial, testing against alternatives μ_1 (respectively Σ_1) as described above with $\sigma_{ptb} = 0.01$.

b) *Exponential family*: For the exponential family dataset, we use the random variable $\mathbf{x} \in \mathbb{R}^d$ distributed according to the un-normalized pdf

$$p_\tau(\mathbf{x}) \propto \exp \left\{ -\tau \left(\sum_{i=1}^d x_i^4 + \sum_{1 \leq i \leq d, i \leq j \leq d} x_i^2 x_j^2 \right) \right\}, \quad (21)$$

where $\tau \in \mathcal{T} \subset \mathbb{R}^+$ is the model parameter. This subfamily of the exponential family correspond to pairwise interaction graphical models [21]. We first consider the hypothesis test $\mathcal{H}_\infty : \tau = \tau_\infty = 1$ versus $\mathcal{H}_1 : \tau = \tau_1 = \tau_0 + \tau_{ptb}$, with $\tau_{ptb} = 0.01$. Hamiltonian Monte Carlo (HMC) is used to generate samples from the un-normalized density functions. In order to perform LRT, we compute the normalizing constant by numerical integration.

c) *RBM*: We also consider the RBM [7] model which is defined based on an undirected bi-partite graphical model consisting of hidden and visible variables. The Gauss-Bernoulli RBM has binary-valued hidden variables $\mathbf{h} \in \{0, 1\}^{d_h}$ and real-valued visible variables $\mathbf{x} \in \mathbb{R}^{d_x}$ with joint distribution

$$p(\mathbf{x}, \mathbf{h}) = \frac{1}{Z_\theta} \exp \left\{ - \left(\frac{1}{2} \sum_{i=1}^{d_x} \sum_{j=1}^{d_h} \frac{x_i}{\sigma_i} W_{ij} h_j + \sum_{i=1}^{d_x} b_i x_i + \sum_{j=1}^{d_h} c_j h_j - \frac{1}{2} \sum_{i=1}^{d_x} \frac{x_i^2}{\sigma_i^2} \right) \right\},$$

where $\theta = (\mathbf{W}, \mathbf{b}, \mathbf{c})$ are model parameters and Z_θ is the normalizing constant. We set $\sigma_i = 1$ for all $i = 1, \dots, d_x$ in our experiments. The probability of the visible variable \mathbf{x} written as $p(\mathbf{x}) = \sum_{\mathbf{h} \in \{0, 1\}^{d_h}} p(\mathbf{x}, \mathbf{h}) = \frac{1}{Z_\theta} \exp\{-F_\theta(\mathbf{x})\}$, where $F_\theta(\mathbf{x})$ is the free energy given by

$$F_\theta(\mathbf{x}) = \frac{1}{2} \sum_{i=1}^{d_x} (x_i - b_i)^2 - \sum_{j=1}^{d_h} \text{Softplus} \left(\sum_{i=1}^{d_x} W_{ij} x_i + b_j \right). \quad (22)$$

The Softplus function is defined as $\text{Softplus}(t) \triangleq \log(1 + \exp(t))$ with a default scale parameter $\beta = 1$. The corresponding Hyvärinen score $S_{\mathbb{H}}(\mathbf{X}_n, \theta)$ is given by

$$S_{\mathbb{H}}(\mathbf{X}_n, \theta) = \sum_{n=1}^n \sum_{i=1}^{d_x} \left[\frac{1}{2} \left(x_{in} - b_i + \sum_{j=1}^{d_h} W_{ij} \delta_{jn} \right)^2 + \sum_{j=1}^{d_h} W_{ij}^2 \delta_{jn} (1 - \delta_{jn}) - 1 \right],$$

where $\delta_{jn} \triangleq \text{Sigmoid}(\sum_{i=1}^{d_x} W_{ij} x_{in} + b_j)$. The Sigmoid function is defined as $\text{Sigmoid}(t) \triangleq (1 + \exp(-t))^{-1}$. We randomly draw the weight matrix $\mathbf{W}_0 \in \mathbb{R}^{d_x} \times \mathbb{R}^{d_h}$ from the standard Normal distribution. In our experiments, we set the dimension of visible variables to $d_x = 50$ and hidden variables to $d_h = 40$. The weight matrix of the alternative hypothesis is constructed by perturbing elements of \mathbf{W}_0 with i.i.d samples of Normal distribution $\mathcal{N}(0, \sigma_{ptb}^2)$ with $\sigma_{ptb} = 0.01$. Samples of RBMs are drawn using Gibbs sampling with 1000 RBM iterations in order to ensure convergence.

d) *KDD Cup*: For the KDD Cup'99 dataset, the 'normal' traffic network is treated as the null hypothesis, against various types of adversarial network attacks as alternative hypotheses. A Gauss-Bernoulli RBM is trained with all available training data of the 'normal' traffic network to estimate an unnormalized version of the null distribution P_∞ . Hypothesis tests

TABLE I
STATISTICS OF VARIOUS NETWORK TRAFFIC IN KDD CUP'99 DATASET.

normal	neptune	back	teardrop	satan	warezclient
87832	51820	968	918	906	893
ipsweep	smurf	portsweep	pod	nmap	unknown
651	641	416	206	158	177

are conducted against various alternative hypotheses, including 'back', 'ipsweep', 'neptune', and others. The 'unknown' adversarial network attack combines all types of attacks with a dataset size of ≤ 100 . To provide a comprehensive overview, the number of available data points of the network traffic in the KDD Cup'99 dataset are depicted in Table I.

We conducted two sets of experiments. In the first set, we explicitly use the *un-normalized* null (P_∞) and alternative (P_1) distributions from true data distributions of synthetic data. The synthetic data experiments include normal distributions, exponential family, and Gauss-Bernoulli RBM. In the second set of simulations (the Gauss-Bernoulli RBM and KDD Cup'99 datasets), we fit the alternative distribution P_1 using training data of size N , with cold-start from the null distribution. For the null distribution, we use the explicit un-normalized data distribution for the synthetic Gauss-Bernoulli RBM experiment. For the KDD Cup'99 dataset experiment, we fit the unnormalized null distribution with a Gauss-Bernoulli RBM using all the available training data of the 'normal' traffic network. In order to demonstrate the robustness of our results to the sampling of alternative training data, we produced 100 alternative distributions, each trained with N alternative data samples. For each test, one of the alternative distributions is randomly selected. Furthermore, we conducted ablation studies on the training data size N in order to demonstrate the influence of the underfitting/overfitting of the alternative distribution on our large deviation analysis results. This is important because in many practical applications (such as detecting adversarial network attacks), alternative data are much more scarce than the null data.

B. Experimental Results

In our first set of experiments (as described above), we evaluate the performance of the Hyvarinen Score Test (HST) and Likelihood Ratio Test (LRT) for explicit data distributions. These distributions include multivariate normal distributions, the exponential family, and Gauss-Bernoulli Restricted Boltzmann Machines (RBMs). Results from these distributions are presented in Figures 1 to 2. These results are consistent with our theoretical analysis given in Section II. Specifically, as the sample size n in the composite hypothesis tests is increased, both the empirical positive and negative error exponents converge to their corresponding theoretical limits.

In the second set of experiments (as described above), we focus on scenarios where the alternative distribution P_1 is fit using the training data. These results are depicted in Figures 5 through 16. In these experiments, we observed that the empirical positive and negative error exponents occasionally

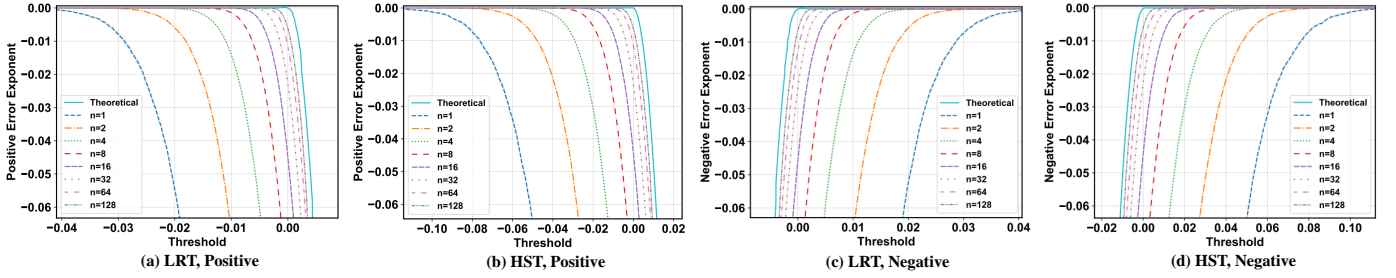


Fig. 1. Large deviation analysis of likelihood-based and score-based hypothesis testing for multivariate normal distribution with perturbation on μ and $\sigma_{ptb} = 0.01$.

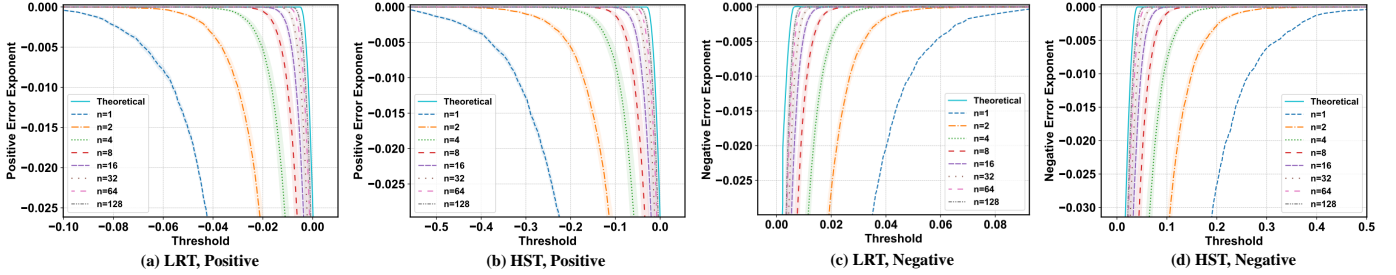


Fig. 2. Large deviation analysis of likelihood-based and score-based hypothesis testing for multivariate normal distribution with perturbation on σ and $\sigma_{ptb} = 0.01$.

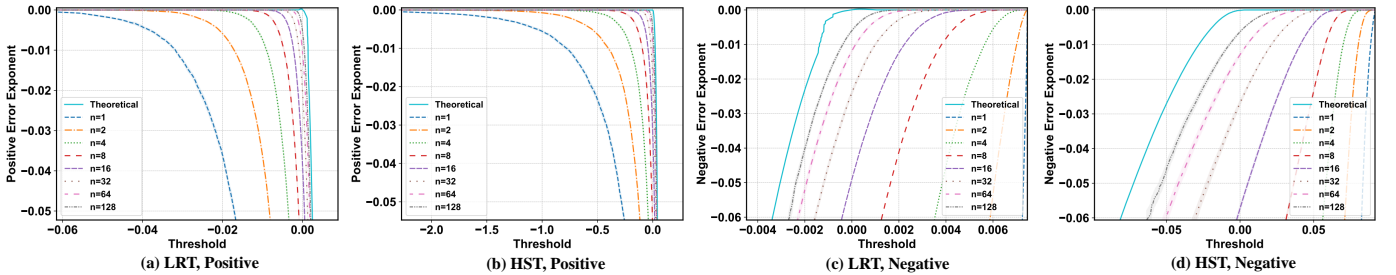


Fig. 3. Large deviation analysis of likelihood-based and score-based hypothesis testing for exponential family with perturbation on τ and $\sigma_{ptb} = 0.01$.

exceed the theoretical limits as n grows large. However, this trend disappears as the number of samples N (used to fit the alternative distribution) increases. As N increases (for instance from 10 to 100 in Figure 5 and from 10 to *All* in Figure 6), the empirical results more frequently adhere to the theoretical limits, aligning with our expectation. Furthermore, we also observe that when N increases, the empirical error exponent becomes more convex. These results suggest that a more accurately fitted alternative distribution facilitates the convergence of the empirical error exponents towards the theoretical limits. Further research could investigate the influence of the fitting accuracy of the alternative distribution on the applicability and effectiveness of the large deviation analysis.

VIII. CONCLUSION

In this work, we analyzed the performance of score-based hypothesis testing method [1]. We derived upper bounds on Type I and II error probabilities, and proved that the exponents of our error bounds become precise in large sample size regimes. We calculated these error exponents numerically for a variety of scenarios of interest. Our experiments using both

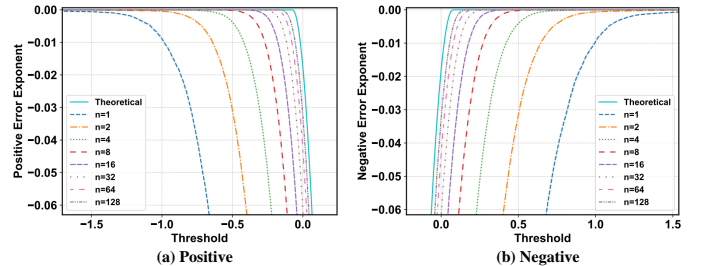


Fig. 4. Large deviation analysis of score-based hypothesis testing for Gauss-Bernoulli RBM with perturbation on W and $\sigma_{ptb} = 0.01$.

synthetic and real-world data demonstrated that the empirical error exponents follow our theoretical analysis. Future research may focus on the impact of lack of accuracy in fitting the alternative distribution on the applicability and effectiveness of large deviation analysis.

REFERENCES

- [1] S. Wu, E. Diao, K. Elkhailil, J. Ding, and V. Tarokh, "Score-based hypothesis testing for unnormalized mod-

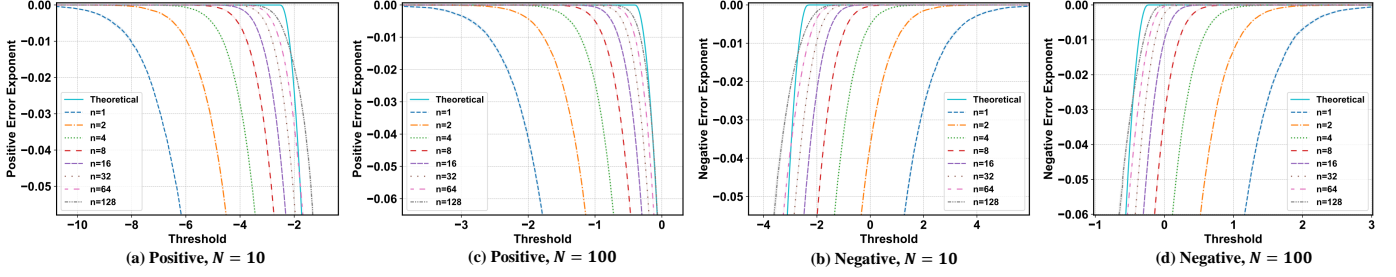


Fig. 5. Large deviation analysis of sore-based hypothesis testing for Gauss-Bernoulli RBM (P_1 fitted with Gauss-Bernoulli RBM and N samples) with perturbation on W and $\sigma_{ptb} = 0.01$.

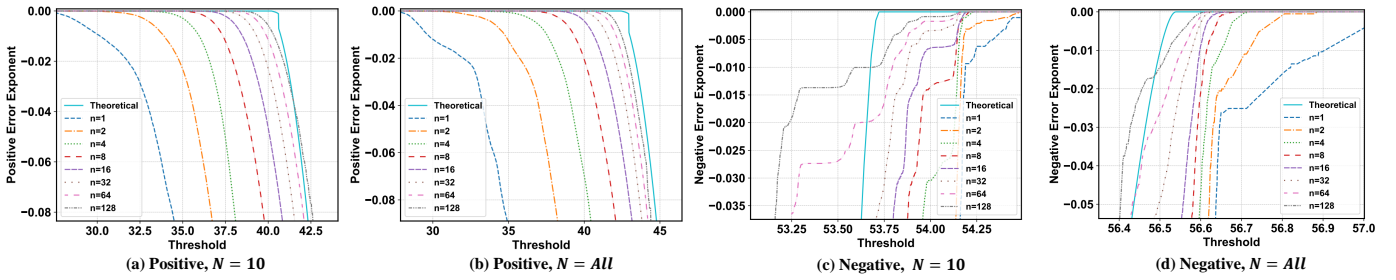


Fig. 6. Large deviation analysis of sore-based hypothesis testing for 'back' attack on KDD Cup'99 dataset (P_1 fitted with Gauss-Bernoulli RBM and N samples).

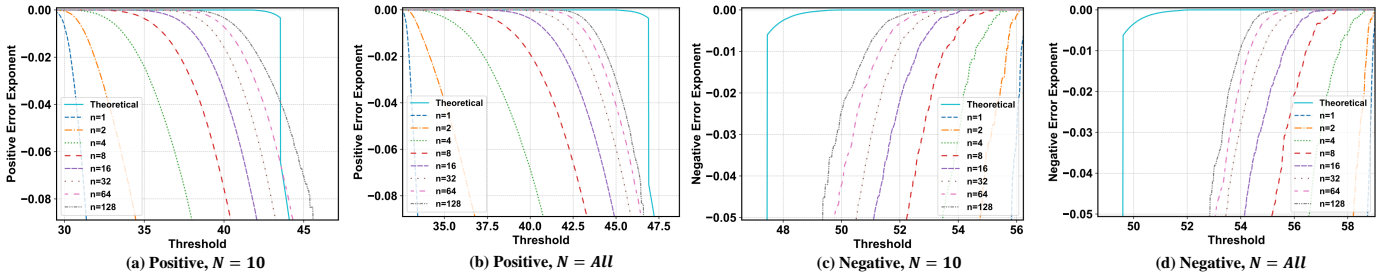


Fig. 7. Large deviation analysis of sore-based hypothesis testing for 'ipsweep' attack on KDD Cup'99 dataset (P_1 fitted with Gauss-Bernoulli RBM and N samples).

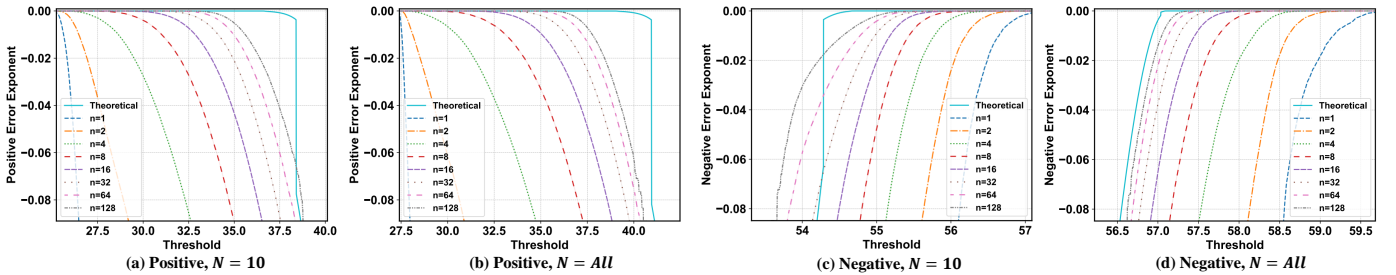


Fig. 8. Large deviation analysis of sore-based hypothesis testing for 'neptune' attack on KDD Cup'99 dataset (P_1 fitted with Gauss-Bernoulli RBM and N samples).

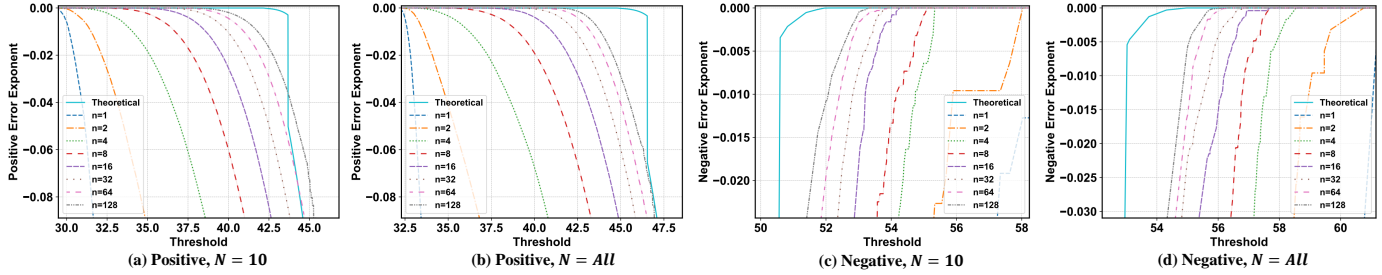


Fig. 9. Large deviation analysis of sore-based hypothesis testing for 'nmap' attack on KDD Cup'99 dataset (P_1 fitted with Gauss-Bernoulli RBM and N samples).

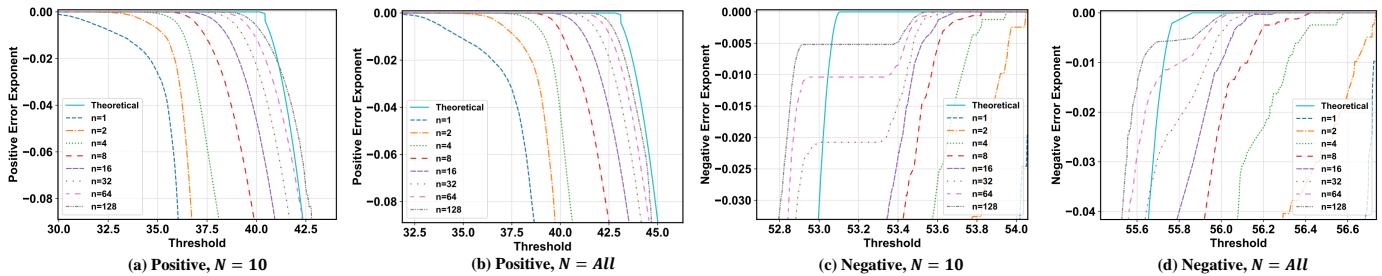


Fig. 10. Large deviation analysis of sore-based hypothesis testing for 'pod' attack on KDD Cup'99 dataset (P_1 fitted with Gauss-Bernoulli RBM and N samples).

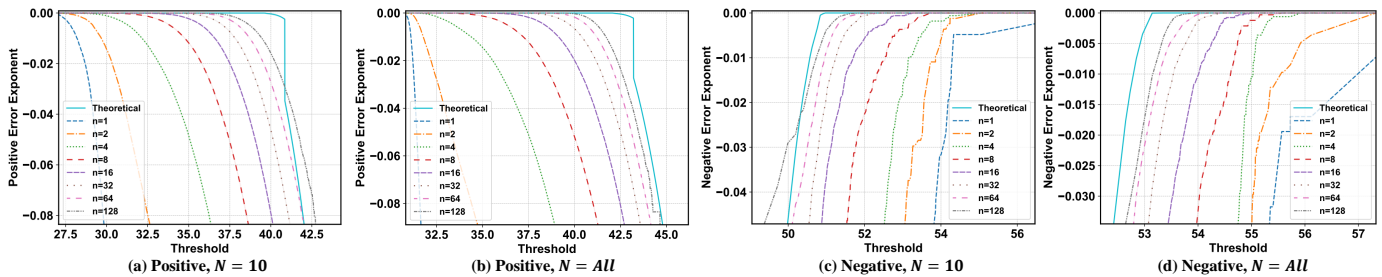


Fig. 11. Large deviation analysis of sore-based hypothesis testing for 'portsweep' attack on KDD Cup'99 dataset (P_1 fitted with Gauss-Bernoulli RBM and N samples).

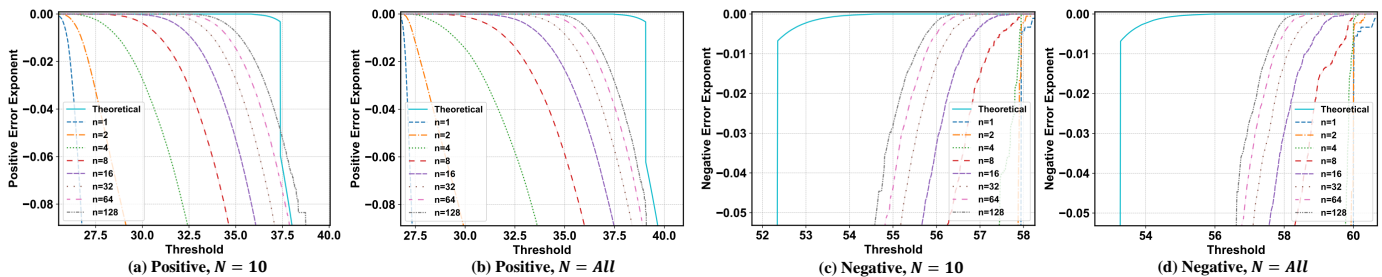


Fig. 12. Large deviation analysis of sore-based hypothesis testing for 'satan' attack on KDD Cup'99 dataset (P_1 fitted with Gauss-Bernoulli RBM and N samples).

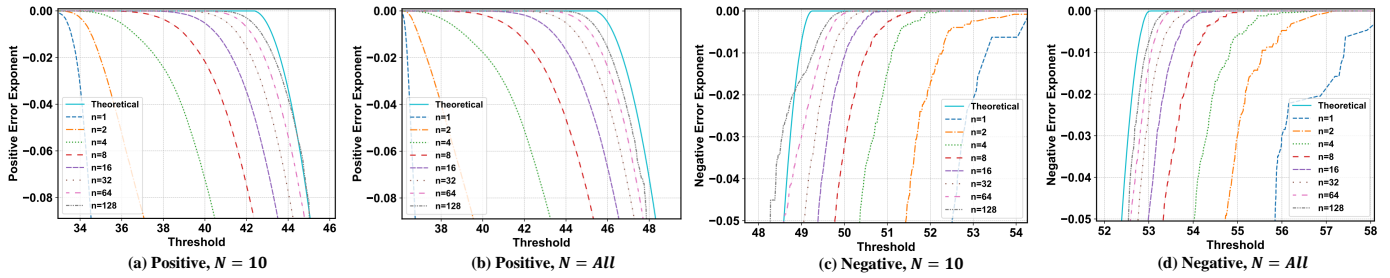


Fig. 13. Large deviation analysis of sore-based hypothesis testing for ‘smurf’ attack on KDD Cup’99 dataset (P_1 fitted with Gauss-Bernoulli RBM and N samples).

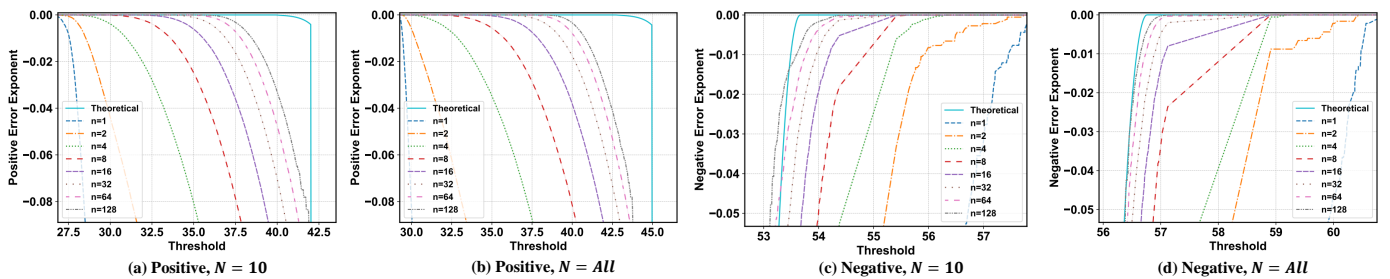


Fig. 14. Large deviation analysis of sore-based hypothesis testing for ‘teardrop’ attack on KDD Cup’99 dataset (P_1 fitted with Gauss-Bernoulli RBM and N samples).

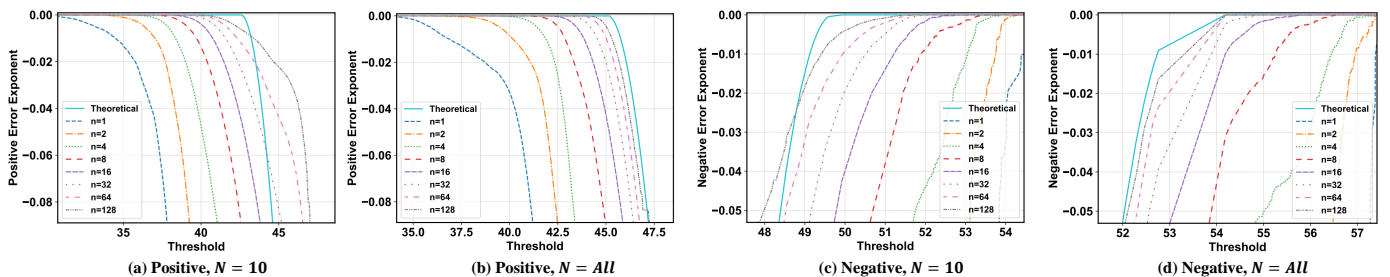


Fig. 15. Large deviation analysis of sore-based hypothesis testing for ‘warezclient’ attack on KDD Cup’99 dataset (P_1 fitted with Gauss-Bernoulli RBM and N samples).

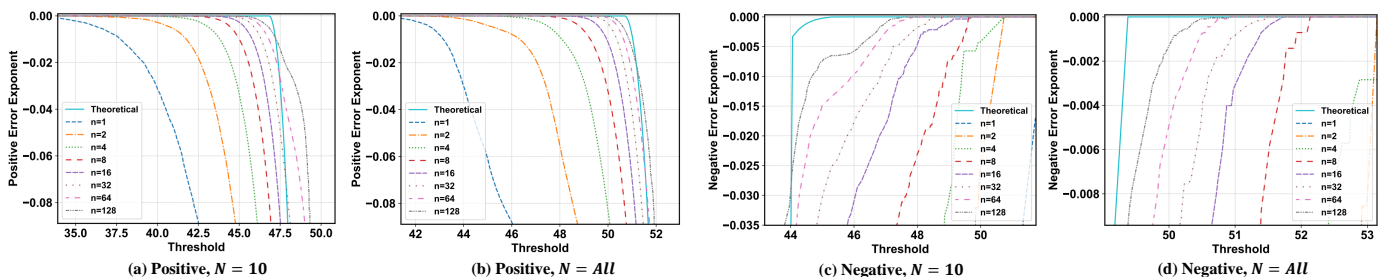


Fig. 16. Large deviation analysis of sore-based hypothesis testing for ‘unknown’ attack on KDD Cup’99 dataset (P_1 fitted with Gauss-Bernoulli RBM and N samples).

- els,” *IEEE Access*, vol. 10, pp. 71 936–71 950, 2022.
- [2] A. Hyvärinen, “Estimation of non-normalized statistical models by score matching,” *J. Mach. Learn. Res.*, vol. 6, no. 4, 2005.
- [3] —, “Some extensions of score matching,” *Comput. Stat. Data Anal.*, vol. 51, no. 5, pp. 2499–2512, 2007.
- [4] Y. Song, J. Sohl-Dickstein, D. P. Kingma, A. Kumar, S. Ermon, and B. Poole, “Score-based generative modeling through stochastic differential equations,” *arXiv preprint arXiv:2011.13456*, 2020.
- [5] A. Vahdat, K. Kreis, and J. Kautz, “Score-based generative modeling in latent space,” *Advances in Neural Information Processing Systems (NeurIPS)*, vol. 34, pp. 11 287–11 302, 2021.
- [6] D. Koller and N. Friedman, *Probabilistic graphical models: principles and techniques*. The MIT Press, 2009.
- [7] Y. LeCun, S. Chopra, R. Hadsell, M. Ranzato, and F. Huang, “A tutorial on energy-based learning,” in *Predicting structured data*. The MIT Press, 2006, vol. 1.
- [8] G. Papamakarios, E. T. Nalisnick, D. J. Rezende, S. Mohamed, and B. Lakshminarayanan, “Normalizing flows for probabilistic modeling and inference,” *J. Mach. Learn. Res.*, vol. 22, pp. 57:1–57:64, 2021.
- [9] R. Cerf and P. Petit, “A short proof of cramer’s theorem in \mathbb{R} ,” *The American Mathematical Monthly*, vol. 118, no. 10, pp. 925–931, 2011.
- [10] A. Dembo and O. Zeitouni, *Large deviations techniques and applications*. Springer Science & Business Media, 2009, vol. 38.
- [11] P. Moulin and V. V. Veeravalli, *Statistical Inference for Engineers and Data Scientists*. Cambridge University Press, 2018.
- [12] E. L. Lehmann, J. P. Romano, and G. Casella, *Testing statistical hypotheses*. Springer, 1986, vol. 3.
- [13] L. Wasserman, *All of nonparametric statistics*. Springer Science & Business Media, 2006.
- [14] S. Wu, E. Diao, T. Banerjee, J. Ding, and V. Tarokh, “Score-based change point detection for unnormalized models,” *International Conference on Artificial Intelligence and Statistics (AISTATS)*, 2023.
- [15] Y. Song and S. Ermon, “Generative modeling by estimating gradients of the data distribution,” *Advances in neural information processing systems*, vol. 32, 2019.
- [16] P. Vincent, “A connection between score matching and denoising autoencoders,” *Neural computation*, vol. 23, no. 7, pp. 1661–1674, 2011.
- [17] S. Wu, E. Diao, T. Banerjee, J. Ding, and V. Tarokh, “Robust quickest change detection for unnormalized models,” *Conference on Uncertainty in Artificial Intelligence (UAI)*, 2023.
- [18] A. Mahmood, J. Oliva, and M. A. Styner, “Multi-scale score matching for out-of-distribution detection,” in *International Conference on Learning Representations*, 2020.
- [19] S. Kulinski, S. Bagchi, and D. I. Inouye, “Feature shift detection: Localizing which features have shifted via conditional distribution tests,” *Advances in neural information processing systems*, vol. 33, pp. 19 523–19 533, 2020.
- [20] R. Lippmann, J. W. Haines, D. J. Fried, J. Korba, and K. Das, “Analysis and results of the 1999 darpa off-line intrusion detection evaluation,” in *International Workshop on Recent Advances in Intrusion Detection*. Springer, 2000, pp. 162–182.
- [21] M. Yu, M. Kolar, and V. Gupta, “Statistical inference for pairwise graphical models using score matching,” *Advances in Neural Information Processing Systems (NeurIPS)*, vol. 29, 2016.